



Modelling of the soft X-ray tungsten spectra expected to be registered by GEM detection system for WEST

Łukasz Syrocki,
Ewa Szymańska,
Katarzyna Słabkowska,
Marek Polasik,
Grzegorz Pestka

Abstract. In the future International Thermonuclear Experimental Reactor (ITER), the interaction between the plasma and the tungsten chosen as the plasma-facing wall material imposes that the hot central plasma loses energy by X-ray emission from tungsten ions. On the other hand, the registered X-ray spectra provide alternative diagnostics of the plasma itself. Highly ionized tungsten emits extremely complex X-ray spectra that can be understood only after exhaustive theoretical studies. The detailed analyses will be useful for proper interpretation of soft X-ray plasma radiation expected to be registered on ITER-like machines, that is, Tungsten (W) Environment in Steady-state Tokamak (WEST). The simulations of the soft X-ray spectra structures for tungsten ions have been performed using the flexible atomic code (FAC) package within the framework of collisional-radiative (CR) model approach for electron temperatures and densities relevant to WEST tokamak.

Key words: X-ray spectra • tokamak • tungsten L, M, N, X-ray lines • GEM detection system

Ł. Syrocki[✉]
Institute of Plasma Physics and Laser Microfusion,
23 Hery Str., 01-497 Warsaw, Poland
and Faculty of Physics, Astronomy and Informatics,
Nicolaus Copernicus University in Toruń,
87-100 Toruń, Poland,
E-mail: lukes@fizyka.umk.pl

E. Szymańska
Faculty of Chemistry,
Nicolaus Copernicus University in Toruń,
87-100 Toruń, Poland

K. Słabkowska, M. Polasik
Institute of Plasma Physics and Laser Microfusion,
01-497 Warsaw, Poland
and Faculty of Chemistry,
Nicolaus Copernicus University in Toruń,
87-100 Toruń, Poland

G. Pestka
Faculty of Physics, Astronomy and Informatics,
Nicolaus Copernicus University in Toruń,
87-100 Toruń, Poland

Received: 25 July 2015
Accepted: 5 February 2016

Introduction

The measurements performed on soft X-ray (SXR) radiations originating from the magnetic fusion plasmas are a standard way to obtain valuable information about the transport of particles in the reactor volume, density, and magnetic configuration [1–5]. Attention focused on tungsten material is associated with the fact that it became a leading candidate for the plasma-facing material in the future International Thermonuclear Experimental Reactor (ITER) and future tokamaks. Since the metallic walls have been installed on many fusion machines, a new problem occurs. This problem is related to the impurities that are released from the divertor walls, that is why it is so highly desirable to fully understand the impact of the plasma impurities and its effects on plasma scenarios. Such contamination could cause radiative collapses and often lead to a disruption, but on the bright side, impurities could also provide alternative diagnostics for plasma parameters [6–9]. X-ray spectra originating from highly ionized tungsten are extremely complex and demand exhaustive theoretical studies that can be specific to a particular tokamak. Such detailed studies will be especially important for proper interpretation of SXR plasma radiation (0.1–20 keV) expected to be registered on Tungsten (W) Environment in Steady-state Tokamak (WEST) and future ITER-like machines.

In this paper, the modelling of the soft L, M, and N X-ray spectra structures for tungsten in high-temperature tokamak plasmas has been performed within the framework of collisional-radiative (CR) model using the flexible atomic code (FAC) package [4, 5, 9, 10] for electron temperatures and densities relevant to WEST tokamak.

Theory – FAC

The simulations have been performed using the FAC package within the framework of the CR model approach [11]. In the package, the full-relativistic Dirac-Fock-Slater iteration method and the configuration interaction method are used to calculate atomic properties, such as the energy levels, and the transition probabilities for radiative transitions and auto-ionization. The cross sections for excitation and ionization by electron impact, and for the inverse processes radiative recombination and dielectronic capture, are then computed in the distorted-wave approximation. Briefly [10], the energy levels of an atomic ion with N electrons are obtained by diagonalising the relativistic effective Hamiltonian H . In atomic units, this reads:

$$(1) \quad H = \sum_{i=1}^N h_D(i) + \sum_{i<j}^N \frac{1}{r_{ij}}$$

where, $h_D(i)$ is the single-electron Dirac Hamiltonian for the potential due to the nuclear charge and the second term accounts for electron-electron interactions, in which r_{ij} is the distance between the i -th and j -th electrons. The basis states $\Phi_{n\kappa}$, which are usually referred to as configuration state functions (CSF), are antisymmetric sums of products of N one-electron Dirac spinors $\phi_{n\kappa m}$

$$(2) \quad \phi_{n\kappa m} = \frac{1}{r} \begin{pmatrix} P_{n\kappa}(r) \chi_{\kappa m}(\theta, \varphi, \sigma) \\ iQ_{n\kappa}(r) \chi_{-\kappa m}(\theta, \varphi, \sigma) \end{pmatrix}$$

where, $\chi_{\kappa m}$ is the usual spin-angular function, n is the principal quantum number, and κ is the relativistic angular quantum number, which is related to the orbital and total angular momentum.

Results

We have performed modelling using the FAC package for the shape of soft X-ray lines of tungsten, which will be useful for the proper design and optimization of the gas electron multiplier (GEM) detector system [12–14], for wide range of photon energies from 0.1 keV to 15 keV, at electron temperatures from 1.0 keV to 5.0 keV and electron densities from $2.5 \times 10^{19} \text{ m}^{-3}$ to $9.0 \times 10^{19} \text{ m}^{-3}$. The selected results of our preliminary modelling for the L, M, and N X-ray line structures of tungsten W^{28+} , W^{37+} , and W^{46+} ions in plasma have been presented in Figs. 1–4.

Figure 1 presents the soft M and N X-ray line structures for tungsten W^{28+} and W^{37+} ions, predicted by the FAC in the 0.1–4.0 keV range of photon energies, at the electron temperature 1.5 keV and electron density $5 \times 10^{19} \text{ m}^{-3}$. We can observe (see

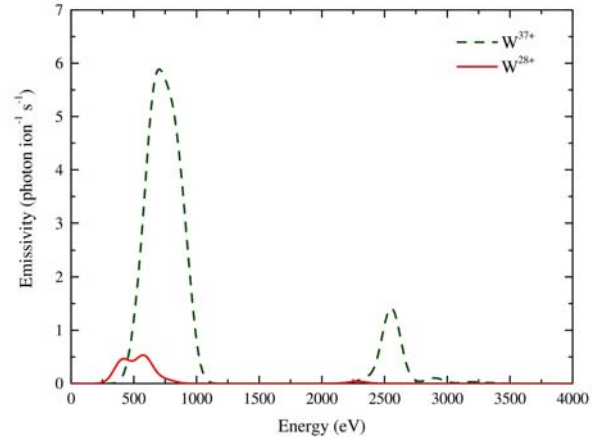


Fig. 1. M and N X-ray line structures for tungsten Pd-like (W^{28+}) and Rb-like (W^{37+}) ions, predicted by the FAC in the 0.1–4.0 keV range of photon energies, at the electron temperature 1.5 keV and electron density $5 \times 10^{19} \text{ m}^{-3}$.

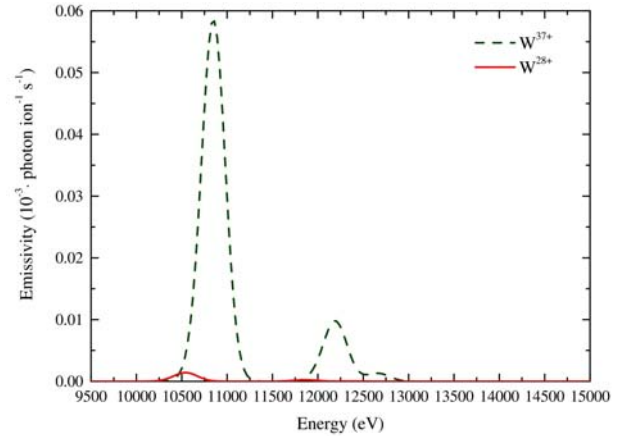


Fig. 2. L X-ray line structures for tungsten Pd-like (W^{28+}) and Rb-like (W^{37+}) ions, predicted by the FAC in the 9.5–15.0 keV range of photon energies, at the electron temperature 1.5 keV and electron density $5 \times 10^{19} \text{ m}^{-3}$.

Fig. 1) that when the ionization increases (compare W^{28+} and W^{37+}), the spectrum is shifted to higher energy. In the range from about 0.2 keV to about 1.1 keV can be seen N X-ray lines with the most intense transitions of the type $5f \rightarrow 4d$ and $5p \rightarrow 4d$. The most intensive peaks for the M X-ray line are located in the region of about 2.2–2.8 keV and the next about 2.8–3.0 keV.

The next figure (Fig. 2) shows the soft L X-ray line structures for tungsten W^{28+} and W^{37+} ions in the 9.5–15.0 keV range of photon energies, at the electron temperature 1.5 keV and electron density $5 \times 10^{19} \text{ m}^{-3}$. We can notice that in the case of L X-ray lines are much lower intensity than the N and M X-ray lines presented in Fig. 1.

The soft N and M X-ray line structures for tungsten W^{37+} and W^{46+} ions in the 0.1–4.0 keV range of photon energies, at the electron temperature 3.5 keV and electron density $5 \times 10^{19} \text{ m}^{-3}$ have been presented in Fig. 3. Same as in the case of Fig. 1, we can observe N X-ray line, but only for W^{37+} ions.

Figure 4 shows the soft L X-ray line structures for tungsten W^{37+} and W^{46+} ions, predicted by the FAC in the 9.5–15.0 keV range of photon energies, at the electron temperature 3.5 keV and electron density

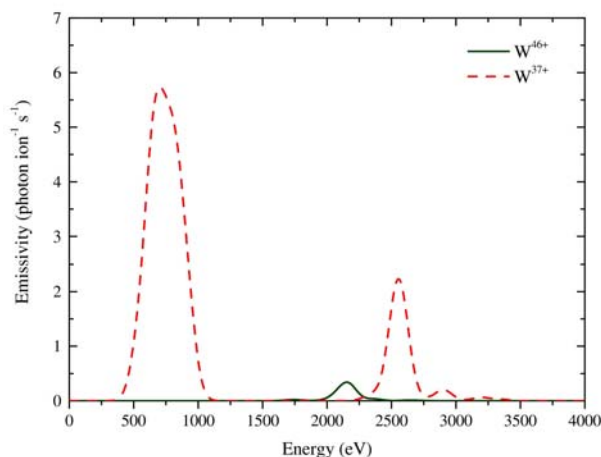


Fig. 3. M and N X-ray line structures for tungsten Rb-like (W^{37+}) and Ni-like (W^{46+}) ions, predicted by the FAC in the 0.1–4.0 keV range of photon energies, at the electron temperature 3.5 keV and electron density $5 \times 10^{19} \text{ m}^{-3}$.

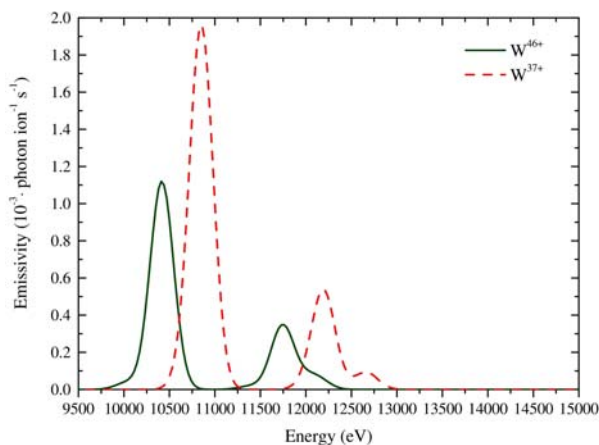


Fig. 4. L X-ray line structures for tungsten Rb-like (W^{37+}) and Ni-like (W^{46+}) ions, predicted by the FAC in the 9.5–15.0 keV range of photon energies, at the electron temperature 3.5 keV and electron density $5 \times 10^{19} \text{ m}^{-3}$.

$5 \times 10^{19} \text{ m}^{-3}$. As can be noticed in the case of L X-ray lines for W^{46+} ions, the most intense transitions are of the type $4d \rightarrow 2p$ and are located in the energy region of about 9.8–10.8 keV. However, in the case of W^{37+} ions, the $5d \rightarrow 2p$ transitions are the most intense (30% more intense than for W^{46+} ions), and moreover, they are shifted to higher energy by about 0.5 keV.

Summary and conclusions

On the basis of results of our modelling for various X-ray lines of tungsten ions (W^{28+} , W^{37+} , and W^{46+}) in plasmas, at electron temperatures and densities relevant to WEST tokamak, we have found that N X-ray lines with the most intense transitions of the type $5f \rightarrow 4d$ and $5p \rightarrow 4d$ are located in the energy range from about 0.4 keV to about 1.1 keV. The most intensive peaks for the M X-ray line are in the region of about 2.5 to 3.0 keV. Moreover, we have found that the L X-ray line are of much lower intensity than the N and M X-ray lines and are located in the energy range from about 10.0 keV to about 13.0 keV.

The results of our modelling presented here will be useful for the proper design and optimization of the GEM detector system [12–14]. The further theoretical studies on the tungsten spectra modelling for different WEST scenarios are in progress, in order to interpret the experimental spectra expected to be registered on WEST. Moreover, our research will be a valuable contribution to develop the diagnostics of plasma parameters in future ITER and DEMO facilities, where tungsten plasma-facing components will be probably implemented.

Acknowledgments. This work has been carried out within the framework of the EUROfusion Consortium and has received funding under the grant agreement no. 633053. This work was also supported by the Polish Ministry of Science and Higher Education for the realization of the international co-financed project under grant no. 2011/01/D/ST2/01286 of the Polish National Science Centre.

References

1. Pütterich, T., Neu, R., Dux, R., Whiteford, A. D., O'Mullane, M. G., & ASDEX Upgrade Team. (2008). Modelling of measured tungsten spectra from ASDEX Upgrade and predictions for ITER. *Plasma Phys. Control. Fusion*, 50, 085016. DOI: 10.1088/0741-3335/50/8/085016.
2. Neu, R., Fournier, K. B., Bolshukhin, D., & Dux, R. (2001). Spectral lines from highly charged tungsten ions in the soft-X-ray region for quantitative diagnostics of fusion plasmas. *Phys. Scr.*, T92, 307. DOI: 10.1238/Physica.Topical.092a00307.
3. O'Mullane, M. G., Summers, H. P., Whiteford, A. D., Meigs, A. G., Lawson, K. D., Zastrow, K. -D., Barnsley, R., Coffey, I. H., & JET-EFDA Contributors. (2006). Atomic modeling and instrumentation for measurement and analysis of emission in preparation for the ITER-like wall in JET. *Rev. Sci. Instrum.*, 77, 10F520. <http://dx.doi.org/10.1063/1.2236278>.
4. Ralchenko, Y., Tan, J. N., Gillaspay, J. D., & Pomeroy, J. M. (2006). Accurate modeling of benchmark x-ray spectra from highly charged ions of tungsten. *Phys. Rev. A*, 74, 042514. <http://dx.doi.org/10.1103/PhysRevA.74.042514>.
5. Clementson, J., Beiersdorfer, P., Brown, G. V., & Gu, M. F. (2010). Spectroscopy of M-shell x-ray transitions in Zn-like through Co-like W. *Phys. Scr.*, 81, 015301. DOI: 10.1088/0031-8949/81/01/015301.
6. Ślabkowska, K., Polasik, M., Szymańska, E., Starosta, J., Syrocki, Ł., Rządkiwicz, J., & Pereira, N. R. (2014). Modeling of the L and M x-ray line structures for tungsten in high-temperature tokamak plasmas. *Phys. Scr.*, T161, 014015. DOI: 10.1088/0031-8949/2014/T161/014015.
7. Ślabkowska, K., Polasik, M., Syrocki, Ł., Szymańska, E., Rządkiwicz, J., & Pereira, N. R. (2015). Modeling of the M X-ray line structures for tungsten and L X-ray line structures for molybdenum. *J. Phys.-Conf. Ser.*, 583, 012031. DOI: 10.1088/1742-6596/583/1/012036.
8. Ślabkowska, K., Rządkiwicz, J., Syrocki, Ł., Szymańska, E., Shumack, A., Polasik, M., Pereira, N. R., & JET Contributors. (2015). On the interpretation of high-resolution x-ray spectra from JET with

- an ITER-like wall. *J. Phys. B-At. Mol. Opt. Phys.*, **48**, 144028. DOI: 10.1088/0953-4075/48/14/144028.
9. Beiersdorfer, P., Clementson, J., Dunn, J., Gu, M. F., Morris, K., Podpaly, Y., Wang, E., Bitter, M., Feder, R., Hill, K. W., Johnson, D., & Barnsley, R. (2010). The ITER core imaging x-ray spectrometer. *J. Phys. B-At. Mol. Opt. Phys.*, **43**, 144008. DOI: 10.1088/0953-4075/43/14/144008.
 10. Gu, M. F. (2008). The flexible atomic code. *Can. J. Phys.*, **86**(5), 675–689. DOI: 10.1139/p07-197.
 11. Kano, K., Suzuki, M., & Akatsuka, H. (2000). Spectroscopic measurement of electron temperature and density in argon plasmas based on collisional-radiative model. *Plasma Sources Sci. Technol.*, **9**, 314. DOI: 10.1088/0963-0252/9/3/309.
 12. Sauli, F. (1997). GEM: A new concept for electron amplification in gas detectors. *Nucl. Instrum. Methods Phys. Res. Sect. A-Accel. Spectrom. Dect. Assoc. Equip.*, **386**, 531–534. DOI: 10.1016/S0168-9002(96)01172-2.
 13. Chernyshova, M., Czarski, T., Dominik, W., Jakubowska, K., Rzadkiewicz, J., Scholz, M., Pozniak, K., Kasproicz, G., & Zabolotny, W. (2014). Development of GEM gas detectors for X-ray crystal spectrometry. *JINST*, **9**, C03003. DOI: 10.1088/1748-0221/9/03/C03003.
 14. Rzadkiewicz, J., Dominik, W., Scholz, M., Chernyshova, M., Czarski, T., Czyrkowski, H., Dabrowski, R., Jakubowska, K., Karpinski, L., Kasproicz, G., Kierzkowski, K., Pozniak, K., Salapa, Z., Zabolotny, W., Blanchard, P., Tyrrell, S., Zastrow, K. -D., & JET EFDA Contributors. (2013). Design of T-GEM detectors for X-ray diagnostics on JET. *Nucl. Instrum. Methods Phys. Res. Sect. A-Accel. Spectrom. Dect. Assoc. Equip.*, **720**, 36–38. DOI: 10.1016/j.nima.2012.12.041.